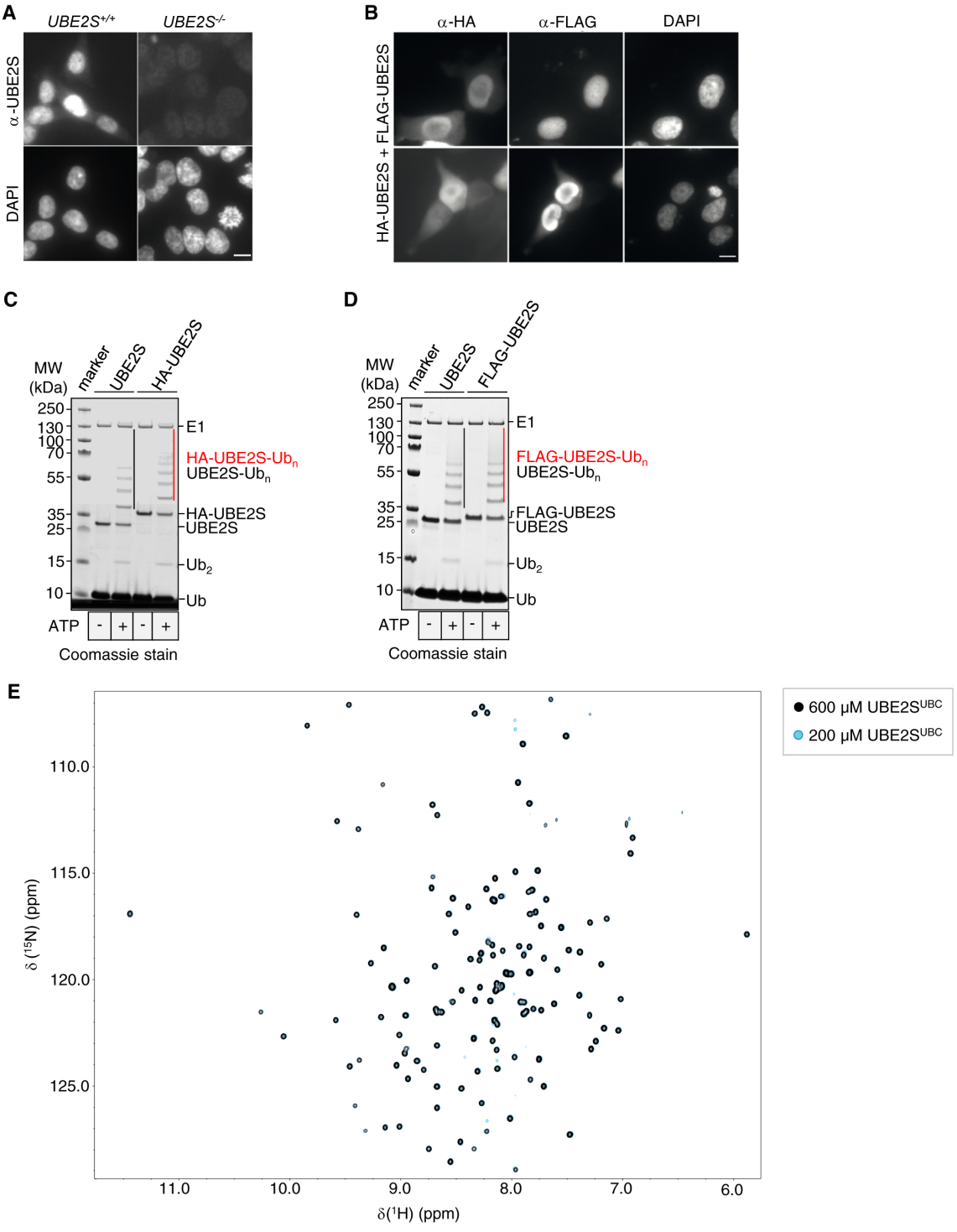

fig. S1. Characterization of UBE2S colocalization and self-association
(A) UBE2S knock-out validation: immunostaining of endogenous UBE2S in HCT116 wild-type (*UBE2S*$^{+/+}$) and UBE2S knock-out cells (*UBE2S*$^{-/-}$) (N=2 independent experiments); scale bar: 10 μm. (B) Immunostaining for FLAG and HA epitopes in HCT116 *UBE2S*$^{-/-}$ cells, co-transfected with plasmids encoding HA-UBE2S and FLAG-

UBE2S (as used for PLAs) (N=4 independent experiments); scale bar: 10 μm. (C, D) Representative in vitro activity assay comparing auto-ubiquitination and the formation of unanchored ubiquitin chains by untagged with HA-tagged (C) and FLAG-tagged (D) UBE2S, respectively, in the absence of the APC/C by SDS-PAGE and Coomassie staining (N=3 independent experiments). Autoubiquitination products formed by the untagged and tagged proteins are indicated by black and red lines, respectively. (E) Superposition of representative $^{1}H^{15}N$-HSQC spectra of $UBE2S^{UBC}$, recorded at 600 μM (black) and 200 μM (blue) protein concentration (N=2 independent experiments).

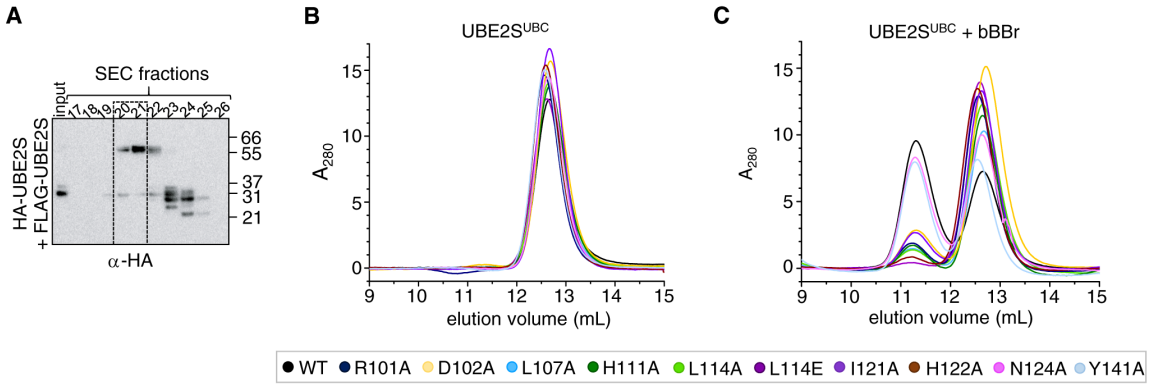

fig S2. Characterization of UBE2S crosslinking in cells and in vitro

(A) Anti-HA immunoblot of SEC fractions of mitotically-enriched, bBBr-treated extract from RPE-1 cells stably expressing Tet-induced HA-UBE2S and transiently expressing FLAG-UBE2S (N=3 independent experiments). For the corresponding anti-FLAG immunoblot, see Fig. 2K. (B) Comparative SEC analyses of purified UBE2S^{UBC} wild-type (analogous to Fig. 2C) and the indicated dimer interface variants at a protein concentration of 40 µM (N=2 independent experiments). (C) Analogous analyses as in (B) after incubation of the individual proteins with 60 µM bBBr for 40 minutes and quenching with NEM (N=2 independent experiments).

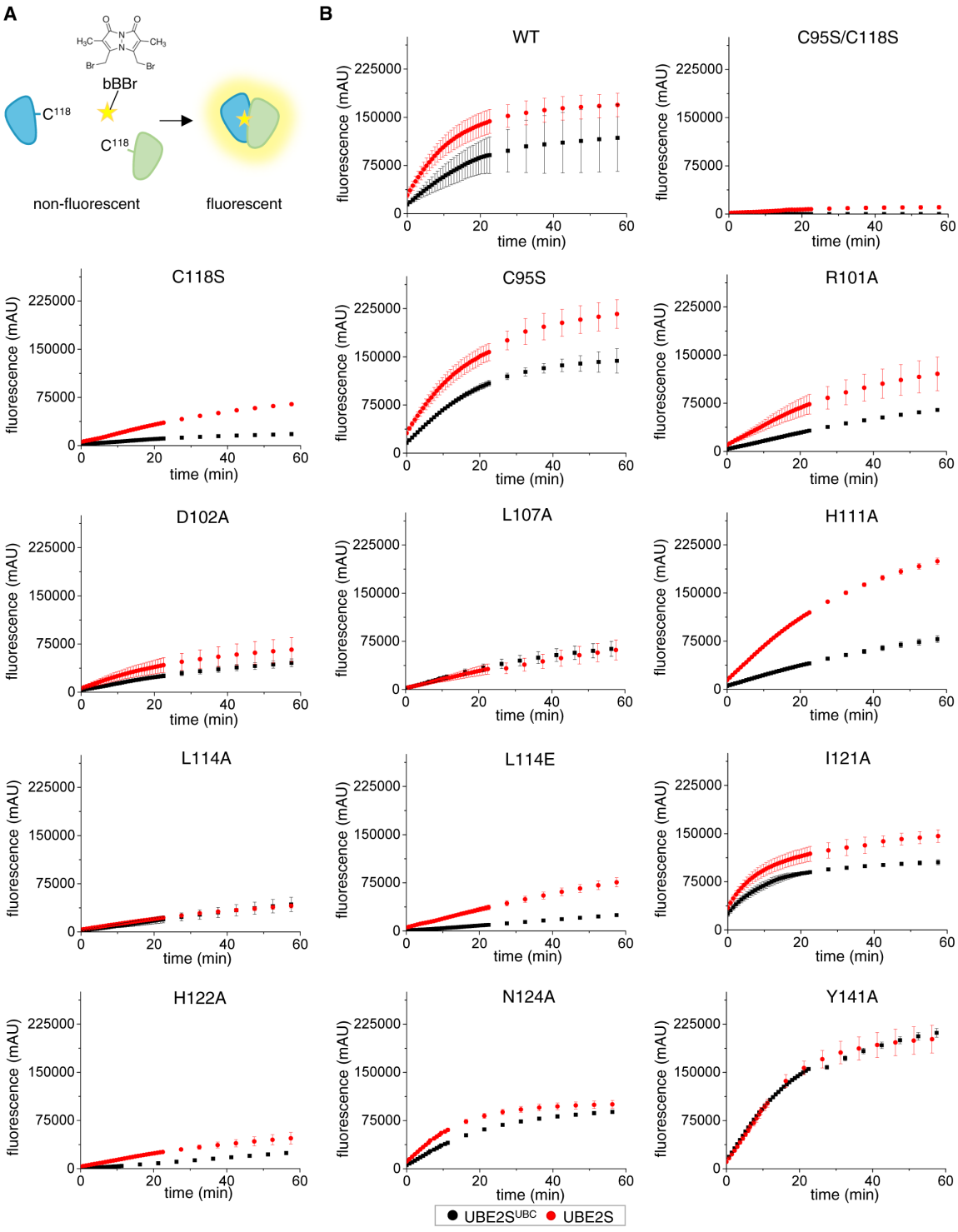

fig. S3. bBBr-based crosslinking kinetics of UBE2S dimer interface variants

(A) Cartoon of the crosslinking reaction. The star represents the crosslinker, bBBr (structure shown above), which becomes fluorescent upon reacting with two thiol groups. (B) Fluorescence intensities plotted over time for the bBBr-based crosslinking of purified wild-type UBE2S^{UBC} (black) and UBE2S (red), respectively, and 13 variants of each. The

mean and SD are plotted (N=3 independent experiments). To determine the crosslinking rates (Fig. 3B) three technical replicates of the measurement triplicates were performed and the initial, linear region of the averaged data fitted by linear regression.

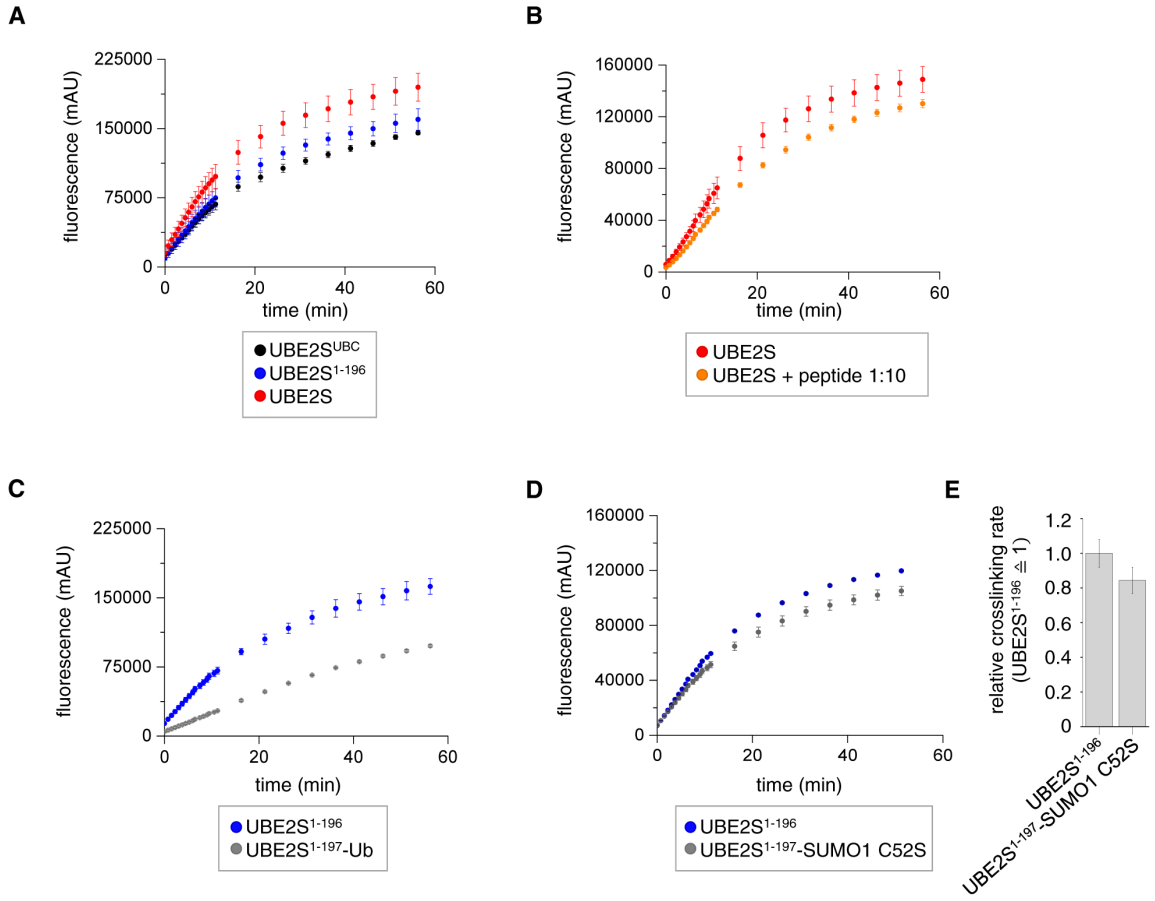

fig. S4. bBBr-based crosslinking kinetics of additional UBE2S variants
(A-D) Fluorescence intensities plotted over time. The bBBr-based crosslinking reactions were performed and analyzed analogously to fig. S3B. (A) Comparison of the crosslinking propensities of UBE2S variants of different length: UBE2S^{UBC} (residues 1-156), UBE2S$^{1-196}$, and full-length UBE2S (N=3 independent experiments). (B) Crosslinking of UBE2S in the presence of a C-helix-derived peptide (residues 197-222), added in trans at the specified molar ratio (N=3 independent experiments). (C) Comparison of the crosslinking propensities of UBE2S$^{1-196}$ with an engineered UBE2S-ubiquitin fusion protein (UBE2S$^{1-197}$-Ub) (N=3 independent experiments). (D) Comparison of the crosslinking propensities of UBE2S$^{1-196}$ with an engineered UBE2S-SUMO1 fusion protein (UBE2S$^{1-197}$-SUMO1 S52A). (E) Quantification of the relative crosslinking rates monitored in (D). The mean and SD are plotted (N=3 independent experiments). For details, see fig. S3B.

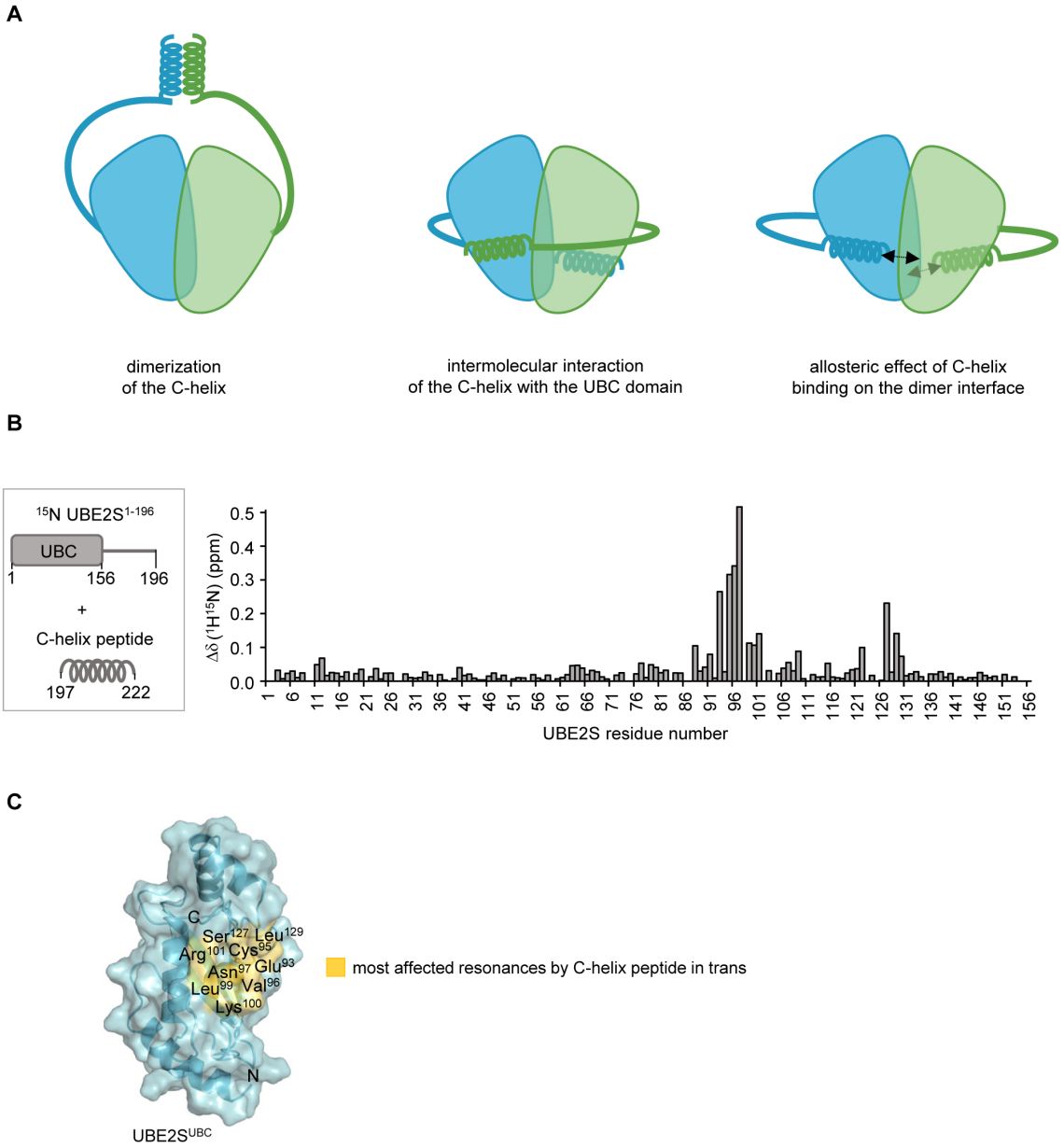

fig. S5. Effect of the C-helix on the UBC domain of UBE2S

(A) Alternative models of how the C-helix may enhance dimerization: dimerization of the C-helix (left); inter-subunit interactions of the C-helix with the UBC domain in the context of the dimer (middle); or allosteric effects on the dimer interface elicited by interactions of the C-helix with the UBC domain in cis (right). (B) Weighted, combined chemical shift perturbations, $\Delta\delta(^{1}H^{15}N)$, of resonances in $UBE2S^{UBC}$ induced by addition of a C-helix-derived peptide (residues 197-222 of UBE2S) to $UBE2S^{1-196}$, plotted over the residue number. The data were measured for a mixture of 200 µM ^{15}N-enriched $UBE2S^{1-196}$ with 6.5 mM peptide (N=1 independent experiment). (C) Cartoon and surface representation of a $UBE2S^{UBC}$ monomer (extracted from PDB: 6S98, this study) with a mapping of the most affected resonances from the experiment in (B) ($\Delta\delta(^{1}H^{15}N) \geq 0.1$ ppm; yellow). The N- and C-termini of the protein are labelled.

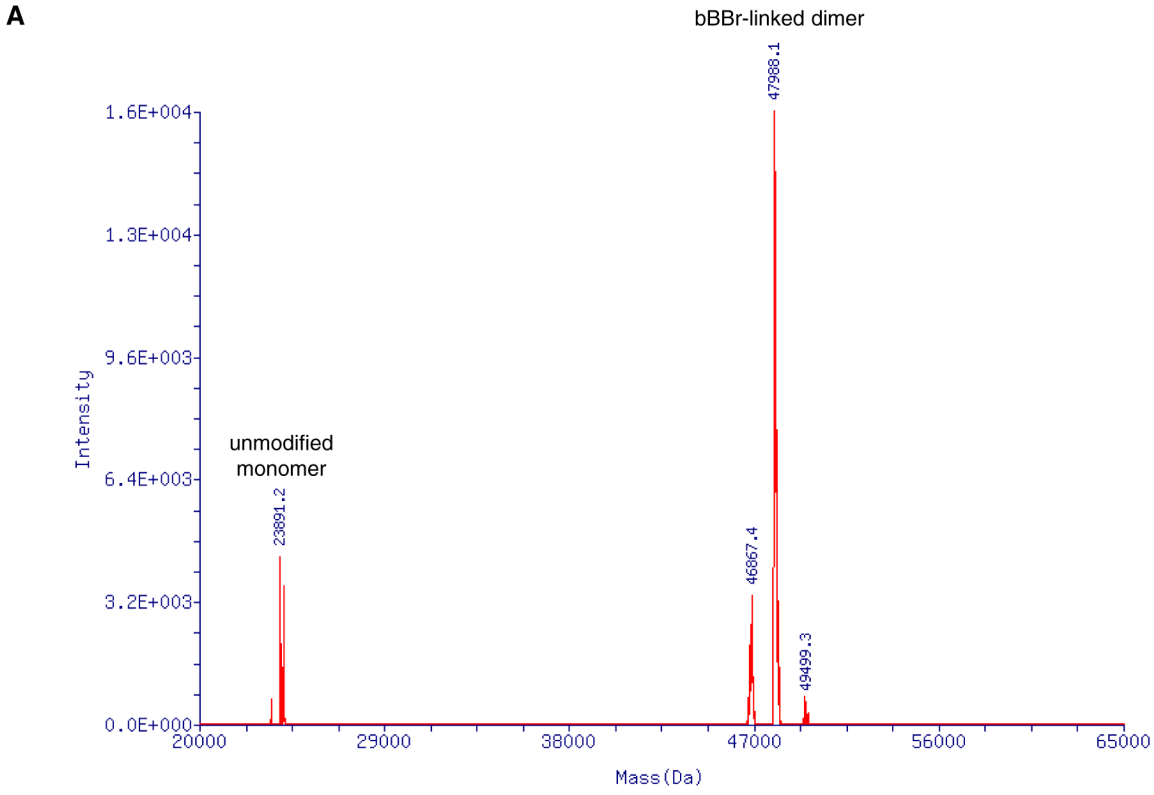
A
bBBr-linked dimer
47908.1
unmodified
monomer
23891.2
46867.4
49499.3
1.6E+004
1.3E+004
9.6E+003
6.4E+003
3.2E+003
0.0E+000
Intensity
20000
29000
38000
47000
56000
65000
Mass(Da)

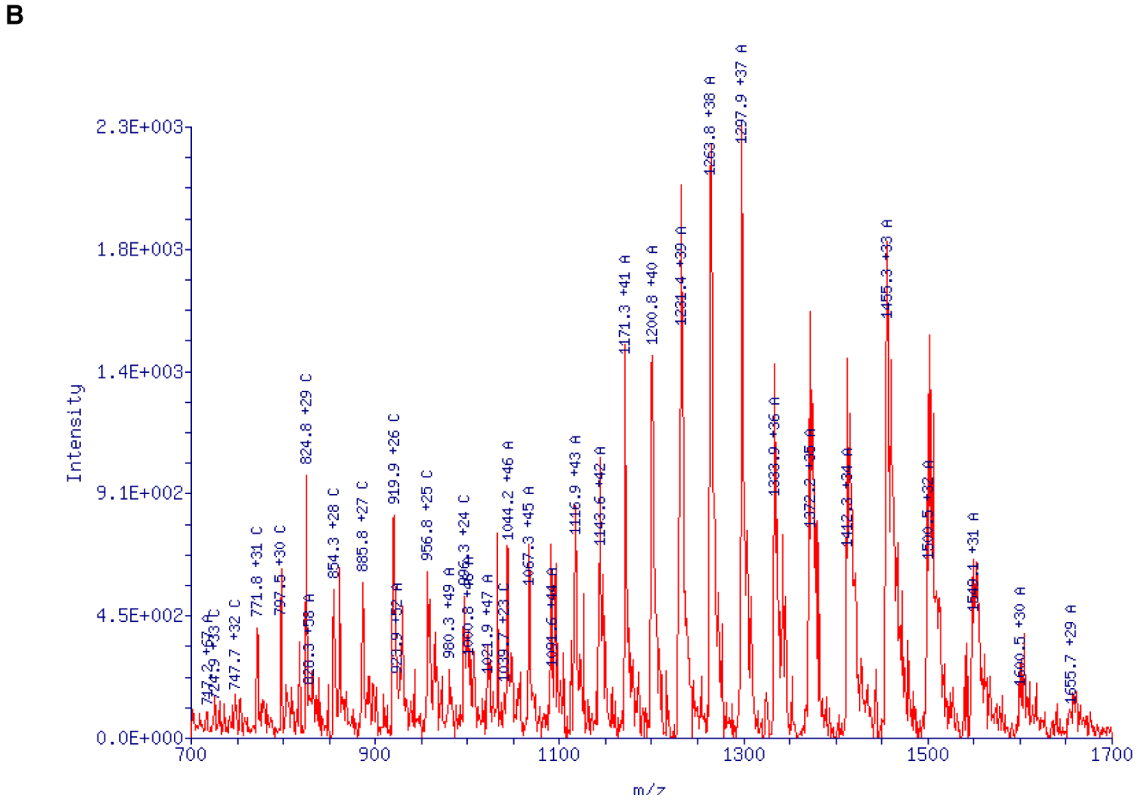
B
2.3E+003
1.8E+003
1.4E+003
9.1E+002
4.5E+002
0.0E+000
Intensity
700
900
1100
1300
1500
1700
m/z

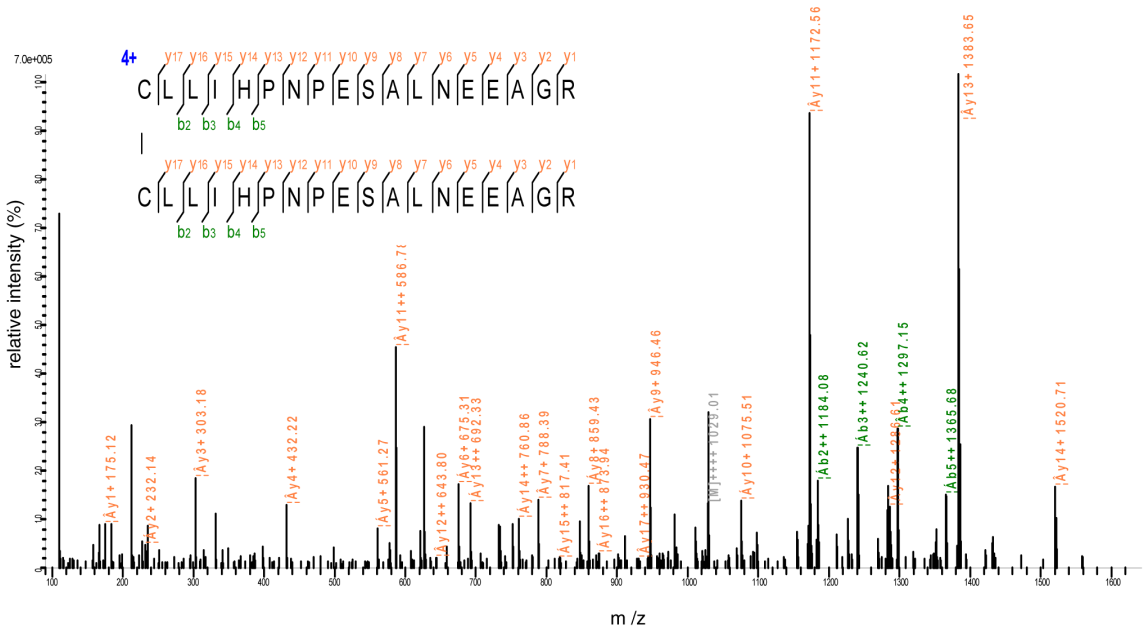

fig. S6. Mass spectrometric analyses of bBBr-based UBE2S crosslinking
(A) Deconvoluted denaturing, intact ESI-mass spectrum of the bBBr-based crosslinking reaction from which the UBE2S dimer was purified. The peak at a MW of 23891.2 Da represents unmodified, monomeric UBE2S (theoretical MW of 23845.0 Da plus two sodium ions); the peak at 47988.1 Da represents the bBBr-crosslinked UBE2S dimer (theoretical MW of 47878.3 Da plus several cations) (N=1 independent experiment). (B) Original ESI data of the deconvoluted spectrum shown in (A). The masses and scores of the observed ions as well as their absolute and relative intensities are provided in table S1 (N=1 independent experiment). (C) Mapping of the bBBr-crosslinking site(s) within the UBE2S dimer by tryptic digest-based ESI-MS. A representative spectrum for the predominant crosslink is shown (Cys^{118} linkage), annotated with pLabel (http://pfind.ict.ac.cn/software/pLink; (72)) (see table S2) (N=2 independent digests).

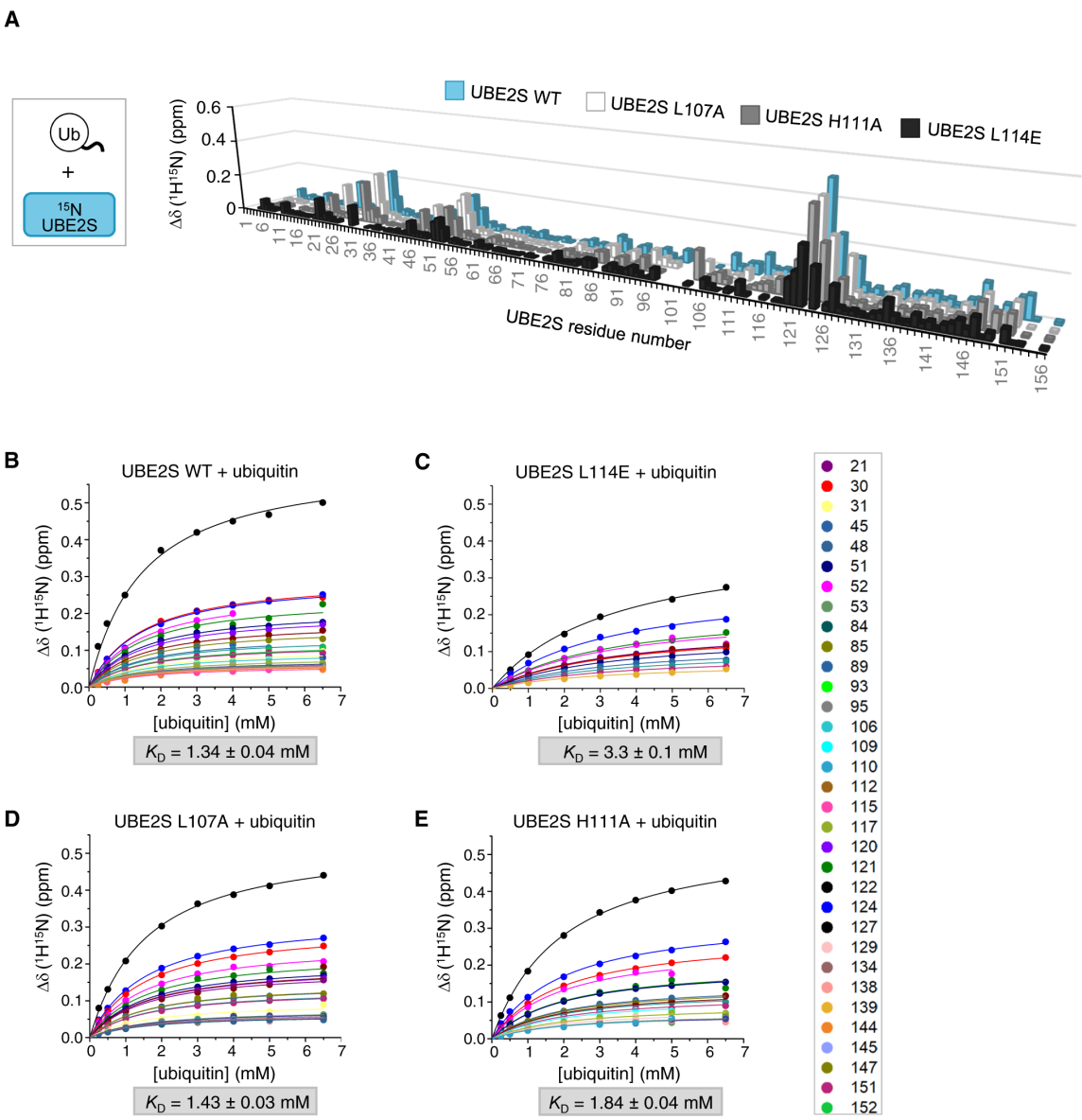

fig. S7. NMR-based comparison of the interactions between UBE2S variants and ubiquitin

(A) Ubiquitin-induced weighted, combined chemical shift perturbations, $\Delta\delta(^{1}H^{15}N)$, of resonances of UBE2S^{UBC} wild-type and the indicated dimer interface variants, plotted over the residue number. The data reflect perturbations upon addition of a 32.5-fold molar excess of ubiquitin (representative of N=3 independent experiments). (B) Ubiquitin-induced perturbations of UBE2S wild-type resonances (with $\Delta\delta(^{1}H^{15}N) \geq 0.048$ ppm at the highest ubiquitin concentration), plotted over the ubiquitin concentration and fitted globally to a single-site model. The data for Gly^{52} are incomplete due to line broadening (N=1 independent experiment). (C) Analogous data and fit as in (B) for UBE2S L114E (N=1). (D) Analogous data and fit as in (B) for UBE2S L107A (N=1 independent experiment). (E) Analogous data and fit as in (B) for UBE2S H111A (N=1 independent

experiment). The resonances of Gly^{52} and Ile^{109} experienced line broadening. The specified errors in the dissociation constants (B-E) solely reflect fitting errors.

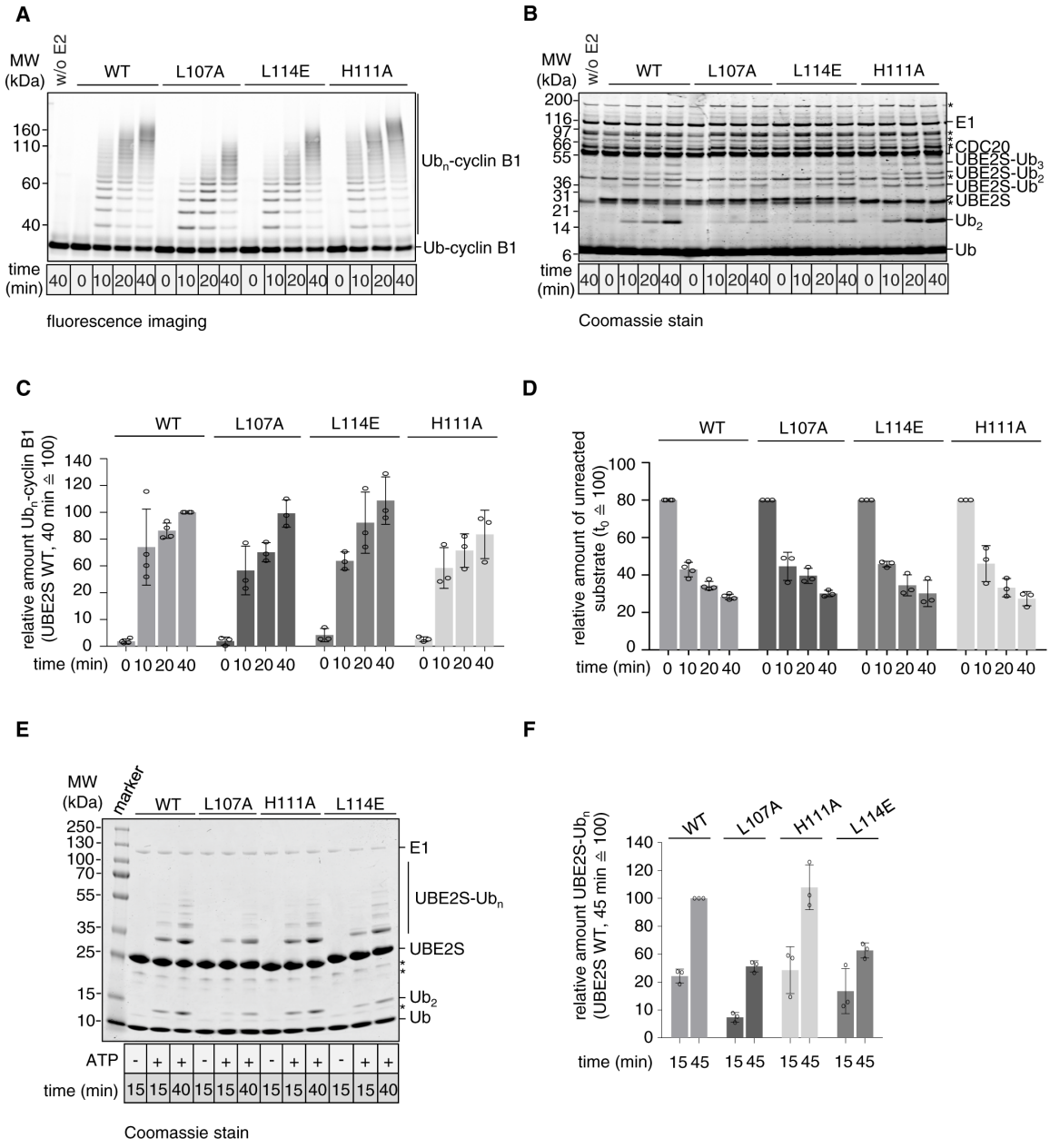

fig. S8. Activity assays with UBE2S wild-type and dimer interface variants

(A, B) Representative assay comparing the activities of UBE2S wild-type with the indicated dimer interface variants in the presence of recombinant APC/C towards fluorophore-labeled ubiquitin-cyclin B1 NTD ('Ub-cyclin B1') by SDS-PAGE and fluorescence imaging (A) and Coomassie staining (B). The use of the ubiquitin-substrate fusion allows UBE2S activity to be monitored without the chain-initiating UBE2C (9). Note that UBE2S H111A runs faster than wild-type UBE2S. (C) Quantification of substrate ubiquitination as shown in (A), based on the amount of Ub_n-cyclin B1 normalized to the activity of wild-type UBE2S at 40 minutes; the mean and SD are plotted (wild-type, N=4; L107A, L114E, H111A, N=3 independent experiments). (D) Complementary quantification of (A) showing the amount of unreacted substrate, normalized to the input

amount at t_0. Note that the differences in total ubiquitination and in the amount of unreacted substrate, respectively, between the wild-type and the indicated dimer interface variants are not significant for any of the time points according to Kruskal-Wallis and Dunnett's multiple comparisons test. (E) Representative assay comparing the auto-ubiquitination activities of UBE2S wild-type and the indicated dimer interface variants in the absence of the APC/C by SDS-PAGE and Coomassie staining (N=3 independent experiments). (F) Quantification of auto-ubiquitination, as shown in (E), normalized to the activity of the wild-type at 45 minutes. Asterisks denote contaminations or degradation.

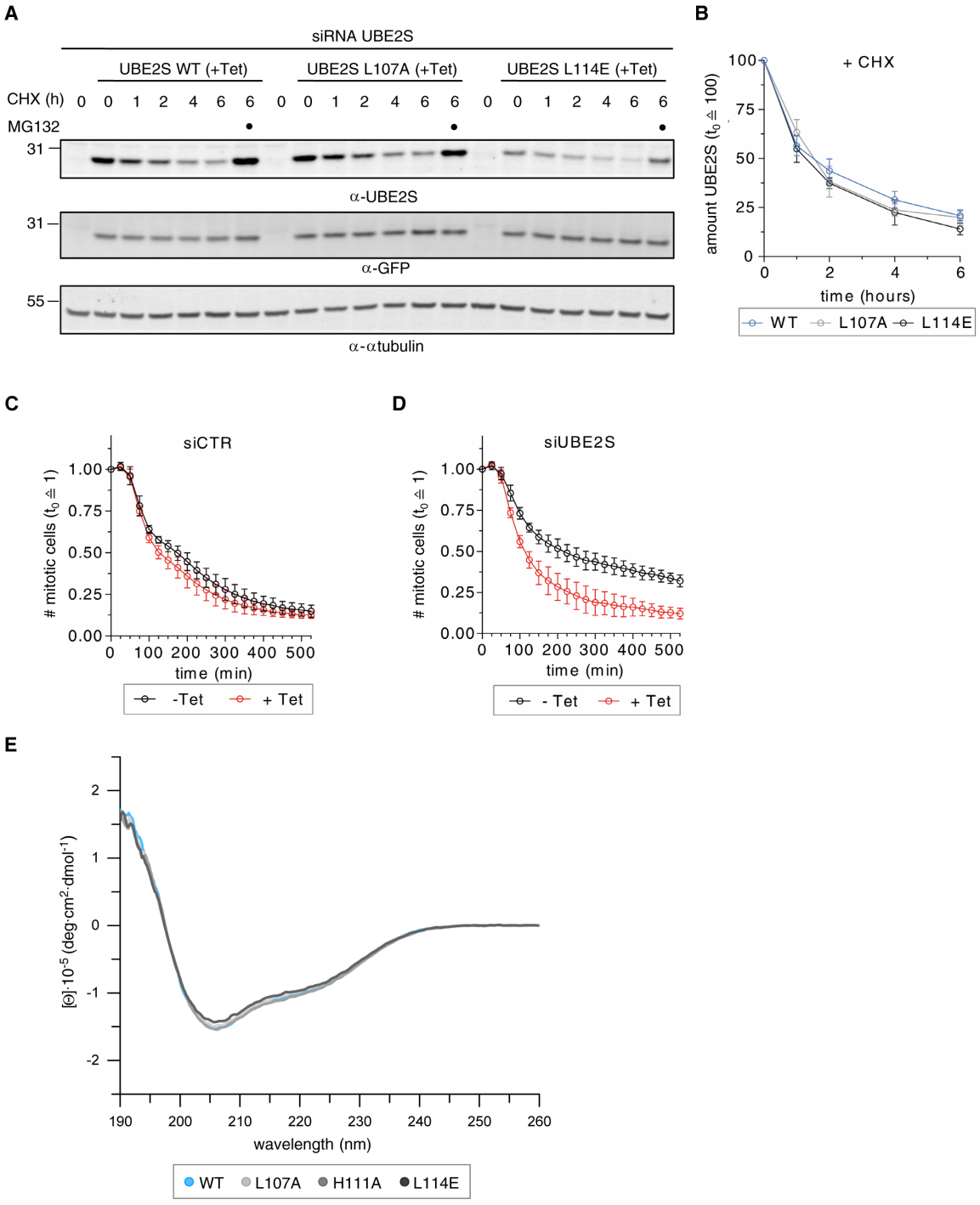

fig. S9. Characterization of UBE2S dimer interface variants in cells and in vitro
(A) Immunoblot of RPE-1 cells upon siRNA-mediated depletion of endogenous UBE2S and Tet-inducible expression of UBE2S wild-type, L107A, and L114E, respectively. Cells were treated with cycloheximide (CHX) or MG132 for different times, as indicated; α-tubulin serves as a loading control. GFP and UBE2S were expressed from the same mRNA. (B) Quantification of the amount of UBE2S in the presence of CHX, normalized to GFP,

based on immunoblotting and fluorescence imaging. The data represent the mean and SD (N=3 independent experiments) from data as shown in (A). The half-lives of UBE2S L107A and L114E are shown in Fig. 6D. (C and D) Quantification of the duration of mitosis after release of cells from a DMA-induced SAC arrest by automated live-cell imaging. Cells were treated with control siRNA (siCTR) (C) and siUBE2S (D), respectively, and complemented with Tet-inducible, untagged wild-type UBE2S. The data represent the mean and SD from 9 measurements (N=3 independent experiments), normalized to the number of mitotic cells at the start of the experiment ($t_0 \triangleq 1$). (E) CD spectra confirming the structural integrity of purified UBE2S wild-type and the indicated variants (N=2 independent experiments)**.**

table S1. Peak list for the deconvoluted mass spectrum shown in fig. S6A
The data for the UBE2S dimer (47988 Da) and monomer (23891 Da) are in bold.

mass (Da)	intensity	score	% relative	% total
47988	**1.61E+04**	**11.15**	**100**	**34.37**
48053.3	8.18E+03	7.66	50.86	17.48
23891	**4.37E+03**	**4.92**	**27.19**	**9.35**
24077.6	3.44E+03	10	21.36	7.34
46867.4	3.36E+03	5.88	20.87	7.17
48139.4	3.24E+03	4.25	20.14	6.92
46789.9	2.08E+03	4.74	12.92	4.44
48213.7	1.49E+03	2.93	9.27	3.19
46733.8	1.22E+03	2.98	7.56	2.6
23966.6	8.09E+02	5.76	5.03	1.73
46956.4	8.00E+02	3.45	4.98	1.71
23473.5	6.48E+02	2.4	4.03	1.39
49499.3	5.91E+02	2.54	3.68	1.26
49610	2.83E+02	2.83	1.76	0.6
46666.3	2.06E+02	2.81	1.28	0.44

table S2. Mapping of bBBr-crosslinking sites in the UBE2S dimer by ESI-MS shown in fig. S6C

The numbers in the columns labeled 'residue 1' and 'residue 2' reflect the positions of the crosslinked cysteine residues, as identified in a pLink search (72). The numbers of crosslink-spectrum matches (CSMs) and the best scores are also provided (smaller score indicates more confident identification); only crosslinks identified with more than 3 CSMs are listed.

				CSMs		best pLink score		CSMs
protein 1	protein 2	residue 1	residue 2	experiment 1	experiment 2	experiment 1	experiment 2	total
splQ1676 3lUBE2S human	splQ1676 3lUBE2S human	95	95	2	5	2.15E-04	1.21E-03	7
splQ1676 3lUBE2S human	splQ1676 3lUBE2S human	118	95	25	31	3.45E-17	3.89E-09	56
splQ1676 3lUBE2S human	splQ1676 3lUBE2S human	118	118	368	361	7.82E-17	8.45E-08	729

table S3. Plasmids, primers, and cloning information

encoded protein	vector	cloning template	cloning primers (5'-> 3')	restriction sites used	reference
recombinant protein expression					
UBE2S^{UBC} (residues 1-156)	pCCA1	-	-	-	(12)
UBE2S^{UBC} C95S	pCCA1	-	-	-	(12)
UBE2S^{UBC} C95A	pCCA1	*UBE2S^{UBC} WT*	F: CCAGTGGCGAGATCGCAGTCAACGTGCTCAAG R: CTTGAGCACGTTGACTGCGATCTCGCCACTGG	-	
UBE2S^{UBC} C118S	pCCA1	-	-	-	(12)
UBE2S^{UBC} R101A	pCCA1	*UBE2S^{UBC} WT*	F: TGCGTCAACGTGCTCAAGGCGGACTGGACGGCTGAGCTG R: CAGCTCAGCCGTCCAGTCCGCCTTGAGCACGTTGACGCA	-	
UBE2S^{UBC} D102A	pCCA1	*UBE2S^{UBC} WT*	F: GTCAACGTGCTCAAGAGGGCCTGGACGGCTGAGCTGGG R: CCCAGCTCAGCCGTCCAGGCCCTCTTGAGCACGTTGAC	-	
UBE2S^{UBC} L107A	pCCA1	*UBE2S^{UBC} WT*	F: GGGACTGGACGGCTGAGGCGGGCATCCGAACGTACTG R: CAGTACGTGTCGGATGCCCGCCTCAGCCGTCCAGTCCC	-	
UBE2S^{UBC} H111A	pCCA1	*UBE2S^{UBC} WT*	F: GAGCTGGGCATCCGAGCAGTACTGCTGACCATC R: GATGGTCAGCAGTACTGCTCGGATGCCCAGCTC	-	
UBE2S^{UBC} L114A	pCCA1	*UBE2S^{UBC} WT*	F: GGCATCCGACACGTACTGGCGACCATCAAGTGCCTGCTG R: CAGCAGGCACTTGATGGTCGCCAGTACGTGTCGGATGCC	-	
UBE2S^{UBC} L114E	pCCA1	*UBE2S^{UBC} WT*	F: GGCATCCGACACGTACTGGAAACCATCAAGTGCCTGCTG R: CAGCAGGCACTTGATGGTTTCCAGTACGTGTCGGATGCC	-	
UBE2S^{UBC} I121A	pCCA1	-	-	-	(12)
UBE2S^{UBC} H122A	pCCA1	*UBE2S^{UBC} WT*	F: CAAGTGCCTGCTGATCGCGCCTAACCCCGAATCTG R: CAGATTCGGGGTTAGGCGCGATCAGCAGGCACTTG	-	
UBE2S^{UBC} Y141A	pCCA1	*UBE2S^{UBC} WT*	F: CTGCTCTTGGAGAACGCGGAGGAGTATGCAGC R: GCTGCATACTCCTCCGCGTTCTCCAAGAGCAG	-	

UBE2S	pCCA1	-	-	-	(12)
UBE2S C95S	pCCA1	-	-	-	(12)
UBE2S C118S	pCCA1	-	-	-	(12)
UBE2S R101A	pCCA1	*UBE2S WT*	F: TGCGTCAACGTGCTCAAGGCGGACTGGACGGCTGAGCTG	-	
			R: CAGCTCAGCCGTCCAGTCCGCCTTGAGCACGTTGACGCA		
UBE2S D102A	pCCA1	*UBE2S WT*	F: GTCAACGTGCTCAAGAGGGCCTGGACGGCTGAGCTGGG	-	
			R: CCCAGCTCAGCCGTCCAGGCCCTCTTGAGCACGTTGAC		
UBE2S L107A	pCCA1	*UBE2S WT*	F: GGGACTGGACGGCTGAGGCGGGCATCCGAACGTACTG	-	
			R: CAGTACGTGTCGGATGCCCGCCTCAGCCGTCCAGTCCC		
UBE2S H111A	pCCA1	*UBE2S WT*	F: GAGCTGGGCATCCGAGCAGTACTGCTGACCATC	-	
			R: GATGGTCAGCAGTACTGCTCGGATGCCCAGCTC		
UBE2S L114A	pCCA1	*UBE2S WT*	F: GGCATCCGACACGTACTGGCGACCATCAAGTGCCTGCTG	-	
			R: CAGCAGGCACTTGATGGTCGCCAGTACGTGTCGGATGCC		
UBE2S L114E	pCCA1	*UBE2S WT*	F: GGCATCCGACACGTACTGGAAACCATCAAGTGCCTGCTG	-	
			R: CAGCAGGCACTTGATGGTTTCCAGTACGTGTCGGATGCC		
UBE2S I121A	pCCA1	-	-	-	(12)
UBE2S H122A	pCCA1	*UBE2S WT*	F: CAAGTGCCTGCTGATCGCGCCTAACCCCGAATCTG	-	
			R: CAGATTCGGGGTTAGGCGCGATCAGCAGGCACTTG		
UBE2S Y141A	pCCA1	*UBE2S WT*	F: CTGCTCTTGGAGAACGCGGAGGAGTATGCAGC	-	
			R: GCTGCATACTCCTCCGCGTTCTCCAAGAGCAG		
$UBE2S^{1-196}$	pCCA1	*UBE2S WT*	F: GAGGGTCCCATGGCCTAGAAGAAGCATGCTGG	-	
			R: CCAGCATGCTTCTTCTAGGCCATGGGACCCTC		
$UBE2S^{1-197}$-Ub	pCCA1	*UBE2S WT*	F: CTGAGGGTCCCATGGCCAAGATGCAGATTTTCGTGAAAC	-	
			R: CGCTCGCCAGCATGCTTCTATTAACCACCACGAAGTCTC		
$UBE2S^{1-197}$ -SUMO1	pCCA1	*$UBE2S^{1-197}$ -Ub*	F: GGCTGAGGGTCCCATGGCCAAGATGTCTGACCAGGAGGCA	-	
			R: GGCCTGCATTCGATGAGGTGCTTATTACACGGTGCTGTGACCCCC		
$UBE2S^{1-197}$ -SUMO1 C52S	pCCA1	*$UBE2S^{1-197}$ -SUMO1*	F: CTCAAAGAATCATACAGCCAAAGACAGGGAGTTCC	-	

			R: GGAACTCCCTGTCTTTGGCTGTATGATTCTTTGAG		
FLAG-UBE2S	pCCA1	*UBE2S WT*	F: GAACAGATTGGTGGCGATTATAAAGATGATGATGATAAAATGAACTCCAACGTGG R: CCACGTTGGAGTTCATTTTATCATCATCATCTTTATAATCGCCACCAATCTGTTC	-	
3xHA-UBE2S	pCCA1	*UBE2S WT*	F: GCTCACAGAGAACAGATTGGTGGGATGTACCCATACGATGTTCCAG R: TGATAGGCCTGCATTCGATGAGGTGCTACAGCCGCCGCAGCGC	-	
His_6-UBE2S^{UBC}	pSKB2 (derived from pET28; Merck)	-	-	-	(12)
His_6-UBE2S	pSKB2 (derived from pET28; Merck)	-	-	-	(12)
PLA					
3xFLAG-Venus	pcDNA5/FRT/TO 3xFLAG	*Venus*	-	KpnI/BamHI	
3xHA-UBE2S L107A	pCS2	*3xHA-UBE2S*	F: GGGACTGGACGGCTGAGGCGGGCATCCGAACGTACTG R: CAGTACGTGTCGGATGCCCGCCTCAGCCGTCCAGTCCC	-	
FLAG-UBE2S L107A	pcDNA5/FRT/TO	*FLAG-UBE2S*	F: GGGACTGGACGGCTGAGGCGGGCATCCGAACGTACTG R: CAGTACGTGTCGGATGCCCGCCTCAGCCGTCCAGTCCC	-	
3xHA-UBE2S L114E	pCS2	*3xHA-UBE2S*	F: GGCATCCGACACGTACTGGCGACCATCAAGTGCCTGCTG R: CAGCAGGCACTTGATGGTCGCCAGTACGTGTCGGATGCC	-	
FLAG-UBE2S L114E	pcDNA5/FRT/TO	*FLAG-UBE2S*	F: GGCATCCGACACGTACTGGCGACCATCAAGTGCCTGCTG R: CAGCAGGCACTTGATGGTCGCCAGTACGTGTCGGATGCC	-	
3xHA-UBE2S H111A	pCS2	*3xHA-UBE2S*	F: GAGCTGGGCATCCGAGCAGTACTGCTGACCATC R: GATGGTCAGCAGTACTGCTCGGATGCCCAGCTC	-	
FLAG-UBE2S H111A	pcDNA5/FRT/TO	*FLAG-UBE2S*	F: GAGCTGGGCATCCGAGCAGTACTGCTGACCATC R: GATGGTCAGCAGTACTGCTCGGATGCCCAGCTC	-	
siRNA-and-rescue					
pCDNA5 FRT/TO-MCS-IRES2-eGFP	pcDNA5/FRT/TO -neo (RRID: Addgene_41000)	*pIRES2-eGFP* (Takara Bio)	-	BamHI/NotI	
UBE2S WT	pCDNA5 FRT/TO-MCS-IRES2-eGFP	wobbled, codon-optimized *UBE2S* (IDT)	-	-	(18)

UBE2S C95S	pCDNA5 FRT/TO-MCS-IRES2-eGFP	wobbled, codon-optimized *UBE2S* (IDT)	F: GGCGAACGGGGAAATAAGCGTGAATGTCTTGAAACG R: CGTTTCAAGACATTCACGCTTATTTCCCCGTTCGCC	-	
UBE2S L107A	pCDNA5 FRT/TO-MCS-IRES2-eGFP	wobbled, codon-optimized *UBE2S* (IDT)	F: ATTGGACCGCGGAAGCCGGGATAAGGCATGTC R: GACATGCCTTATCCCGGCTTCCGCGGTCCAAT	-	
UBE2S H111A	pCDNA5 FRT/TO-MCS-IRES2-eGFP	wobbled, codon-optimized *UBE2S* (IDT)	F: CGCGGAATTAGGGATAAGGGCCGTCTTATTAACG R: CGTTAATAAGACGGCCCTTATCCCTAATTCCGCG	-	
UBE2S L114E	pCDNA5 FRT/TO-MCS-IRES2-eGFP	wobbled, codon-optimized *UBE2S* (IDT)	F: TCCCCGCGGAATTAGGGATAAGGCATGTCTTAGAGACGATAAAATGTTTATTAATACATCCGAATCC R: CCGGGCGCGCCCGGATCCGTACTACTCGCC	SacII/AscI	
cell-based crosslinking					
HA-UBE2S WT	pCDNA5 FRT/TO-MCS-IRES2-eGFP	wobbled, codon-optimized *UBE2S* (IDT)	F: GGGGTACCATGGGCTACCCATACGATGTTCCTGACTATGCGGCGGGTGCGGCGGGTAATAGTAATGTCGAAAATTTGCCGCCCC R: CCGGGCGCGCCCGGATCCGTACTACTCGCC	KpnI	

table S4. Antibodies

application	epitope, or name & conjugation details	product no.	company	species & clonality
PLA & indirect IF	FLAG	14793	Cell Signaling Technology	rabbit polyclonal
	HA	custom-made (73)	Moravian Biotechnology	mouse monoclonal
	UBE2S	11878	Cell Signaling Technology	rabbit monoclonal
	Duolink in situ PLA probe anti-rabbit PLUS	DUO92002	Sigma-Aldrich	donkey polyclonal
	Duolink in situ PLA probe anti-mouse MINUS	DUO92004	Sigma-Aldrich	donkey polyclonal
	anti-rabbit Alexa Fluor 405	A31556	Thermo Fisher Scientific	goat polyclonal
	anti-mouse Alexa Fluor 594	A21203	Thermo Fisher Scientific	donkey polyclonal
	anti-mouse Alexa Fluor 568	A11031	Thermo Fisher Scientific	goat polyclonal
immuno-blotting & IP	CSE1	ab96755	Abcam	rabbit polyclonal
	CSE1	ab54674	Abcam	mouse monoclonal
	FLAG M2	F3165	Sigma-Aldrich	mouse monoclonal
	GFP	custom-made	MPI CBG, Dresden	goat polyclonal
	HA	custom-made (73)	Moravian Biotechnology	mouse monoclonal
	HA	H6533	Sigma-Aldrich	mouse monoclonal
	normal mouse IgG1	sc-3877	Santa Cruz	mouse monoclonal
	poly-histidine	H1029	Sigma-Aldrich	mouse monoclonal
	α-tubulin	T5168	Sigma-Aldrich	mouse monoclonal
	UBE2S	custom-made (18)	Moravian Biotechnology	rabbit polyclonal
	anti-goat IgG, IRDye 800CW conjugate	926-32214	LI-COR Biosciences	donkey polyclonal
	anti-mouse IgG, IRDye 800CW conjugate	926-32212	LI-COR Biosciences	donkey polyclonal
	anti-rabbit IgG, IRDye 800CW conjugate	926-32213	LI-COR Biosciences	donkey polyclonal
	anti-mouse IgG, IRDye 680RD conjugate	926-68072	LI-COR Biosciences	donkey polyclonal
	anti-rabbit IgG, IRDye 680RD conjugate	926-68073	LI-COR Biosciences	donkey polyclonal
	anti-mouse IgG, HRP conjugate	7076	Cell Signaling Technology	horse